Journal of the Royal Statistical Society Series C: Applied Statistics, 2024, **00**, 1–18
https://doi.org/10.1093/jrsssc/qlae021

ROYAL STATISTICAL SOCIETY
DATA | EVIDENCE | DECISIONS
Journal of the Statistics Society
Series C
Applied Statistics

Original Article

Estimating disease transmission in a closed population under repeated testing

Matthew Wascher[1], Patrick M. Schnell[2], Wasiur R. KhudaBukhsh[3], Mikkel B.M. Quam[4], Joesph H. Tien[4,5] and Grzegorz A. Rempała[2,5]

[1]Department of Mathematics, University of Dayton, 300 College Park, Dayton, OH 45469, USA
[2]Division of Biostatistics, College of Public Health, The Ohio State University, 281 W Lane Ave, Columbus, OH 43210, USA
[3]School of Mathematical Sciences, University of Nottingham, University Park, Nottingham NG7 2RD, UK
[4]Division of Epidemiology, College of Public Health, The Ohio State University, 281 W Lane Ave, Columbus, OH 43210, USA
[5]Department of Mathematics, The Ohio State University, 281 W Lane Ave, Columbus, OH 43215, USA

Address for correspondence: Grzegorz A. Rempała, Division of Biostatistics, College of Public Health, The Ohio State University, 281 W Lane Ave, Columbus, OH 43210, USA; Department of Mathematics, The Ohio State University, 281 W Lane Ave, Columbus, OH 43215, USA. Email: rempala.3@osu.edu

Abstract

The article presents a novel statistical framework for COVID-19 transmission monitoring and control, which was developed and deployed at The Ohio State University main campus in Columbus during the Autumn term of 2020. Our approach effectively handles prevalence data with interval censoring and explicitly incorporates changes in transmission dynamics and human behaviour. To illustrate the methodology's usefulness, we apply it to both synthetic and actual student SARS-CoV-2 testing data collected at the OSU Columbus campus in late 2020.

Keywords: dynamic survival analysis, Gibbs sampler, interval censoring

1 Introduction

In response to the COVID-19 pandemic, most American colleges and universities suspended on-campus residence and instruction in early March 2020, opting instead for online instruction (Rapanta et al., 2020). During the following summer, universities needed to decide whether to let students return to on-campus residence and resume in-person instruction. Furthermore, they needed to decide on measures to protect the health and the safety of students, faculty, staff, and the surrounding communities.

By Autumn 2020, multiple modelling and evaluation approaches were developed across the country to assess the feasibility and impact of various mitigation strategies, such as frequent, random testing of asymptomatic individuals, contact tracing and isolation, and capping of in-person class sizes. Some notable approaches involved full-scale agent- or network-based simulations parameterized using information from local epidemics and run forward to yield predictions through the end of an academic term. However, since such simulations often lacked access to reliable transmission data in the campus setting, the predictions carried high uncertainty (see, e.g. Arnst et al., 2022; Cator et al., 2022; Chang et al., 2020; Enright et al., 2021; Frazier et al., 2022; Gressman & Peck, 2020; Hill et al., 2021; McCabe & Donnelly, 2021; Muller & Muller, 2021; Panovska-Griffiths et al., 2020; Rennert et al., 2021; Shah et al., 2022; Zhang et al., 2022).

Received: June 8, 2023. **Revised:** January 3, 2024. **Accepted:** March 22, 2024

Nevertheless, these studies were able to highlight the need for large-scale, frequent, randomized (if not ideally comprehensive) testing of asymptomatic individuals, which was adopted by many colleges and universities that ultimately held in-person instruction during the 2020 Autumn semester.

The Ohio State University (OSU) partially resumed in-person instruction for the Autumn 2020 semester and implemented a battery of strategies to control COVID-19 transmission on campus. The university conducted weekly routine polymerase chain reaction (PCR)-based screening for the SARS-CoV-2 virus among all (mostly undergraduate) students living on campus. In addition to aiding in isolation and contact tracing, trends in these data yielded insight into whether incidence on campus was increasing, decreasing or plateauing.

A naive strategy for estimating prevalence from this testing data could be to use the daily test positive rate (proportion of tests that returned a positive result each day) as an estimate of prevalence, perhaps adjusting for imperfect sensitivity and specificity of the test. However, as argued in our earlier work (Schnell et al., 2024), and also illustrated with the aid of a toy example in Figure 1, the test positive rate is often biased as an estimator of prevalence in the nonremoved population under regular testing schemes such as the one used by OSU. Testing individuals once per week (or a similar block of time) with those testing positive subsequently isolated can induce correlation between the probability of being tested and the probability of being infectious.

Even though it does not appear to be widely recognized that the test positive rate may be biased in repeated testing scenarios, the bias is not the only reason why the test positive rate is a poor choice. The test positive rate also ignores the longitudinal information in the data. In a repeated testing setting where we observe a time series of tests for each individual, the data describe an interval-censored observation of the time each individual first became infectious. Moreover, test positive rates are not suitable for prediction purposes without an underlying transmission model. The test positive rate is commonly interpreted as an estimate of prevalence, both when the goal is to estimate prevalence and when the goal is to use prevalence estimates within a larger modelling framework (Kahanec et al., 2021). If such methods use data from a repeated testing setting, the bias of the test positive rate may be a significant limitation.

In order to monitor COVID-19 transmission among residential students at the OSU on its main campus in Columbus, Ohio, we adopted a mechanistic model-based approach that is not only faithful to the epidemiology of the disease but also adjusts for the testing scheme in a proper way using survival analytic tools. The resulting statistical approach, which we call the interval dynamical survival analysis (IDSA), is our main statistical contribution in this article.

IDSA is a simple yet powerful modelling framework for the analysis of repeated testing data of a closed population. The underlying disease transmission mechanism is described as a discrete-time

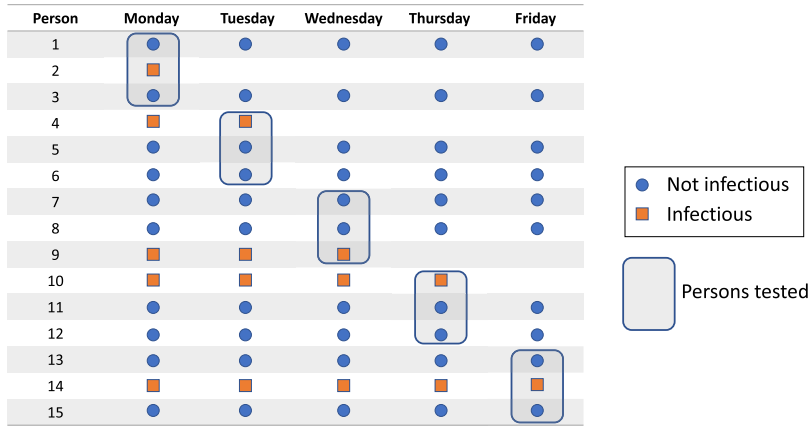

Figure 1. In this example, one-third of the population becomes infectious over the weekend but there are no additional infections during the week. When individuals are tested at random once per week, the test positive rate is one-third each day but the prevalence decreases as infectious individuals are detected and removed. If additional infections occur throughout the week, bias is still present because those ineligible to be tested on a given day have likely had less cumulative exposure hazard since their last negative test, compared with those eligible for testing.

susceptible-exposed-infectious-removed (SEIR) compartmental model, which we fit to the repeated testing data using the so-called dynamical survival analysis (DSA) approach described in KhudaBukhsh et al. (2023, 2020). The goal is to assess the ability of a repeated testing program to control on-campus (residential) outbreaks over the course of a fixed time horizon such as a semester. Our model allows for changes over time in the parameter values governing contact patterns, transmissibility, and social distancing. As the repeat testing data analysed here may be considered interval-censored, we refer to the approach as the *interval* DSA or the IDSA.

We developed a bespoke Markov chain Monte Carlo (MCMC) method to estimate the model parameters. The method, a Metropolis–Hastings (MH)-within-Gibbs algorithm, accounts for imperfect tests and arbitrary testing schedules, and could be of potential statistical interest in its own right. Although the IDSA method was developed in the context of COVID-19, the method is general in that it can be applied to analyse and monitor the transmission of any disease among a closed population based on repeated testing data. Moreover, since the underlying transmission dynamics are described by means of a mechanistic model (the compartmental SEIR model chosen for convenience in this article), the IDSA method can be used for predictive purposes as well.

The remainder of the article is organized as follows. In Section 2, we describe the IDSA model and its approach for parameter estimation and validation. In particular, Sections 2.4 and 2.6 describe the data sources and the process of integrating data into our models. Section 3.2 presents a simulation study illustrating the model's performance. In Section 3.3, we apply the model to data from weekly testing of OSU residential students in Autumn 2020. Finally, some concluding remarks and an overview of related work are given in Section 4. Summary of notation in given in Table A1 in the Appendix.

2 Methods

2.1 Data structure

Repeated testing is performed in an on-campus population. We assume the following:

1. All individuals are tested repeatedly (e.g. weekly), each time on a day of their choice within the fixed testing window.
2. The window between consecutive tests is shorter than the typical natural recovery time of the disease.
3. Upon testing positive, individuals are isolated and removed from the population, perhaps after some delay.

Note that under these assumptions, some infections may still go undetected, either due to imperfect testing (see Section 2.5) or individuals recovering before they are tested. However, we expect that, given a reasonably sensitive test, most infections will be detected under these assumptions.

In the population, we assume to observe all individual test dates, test results (positive or negative), and removal times (for individuals who test positive). A number of organizations (e.g. sports leagues, universities) have used such testing schemes in response to the COVID-19 pandemic (Maloney, 2021; Walke et al., 2020). The OSU tested and collected data from 8 August to 24 November 2020 as part of the university's plan to manage and mitigate COVID-19 cases during the autumn semester with students on campus (OSU Monitoring Team, 2021). The OSU's policy was to test each of $n = 12,567$ students living on campus weekly, keeping in mind that the natural recovery time for COVID-19 is thought to be between 10 and 14 days for the majority of cases (CDC, 2023). In the event of a positive test, the student was isolated for 10 days from the date of the test, in a designated quarantine/isolation (Q/I) location on campus, and contact tracing was initiated. Individuals identified as close contacts of a positive testing individual were quarantined for 14 days. Because the percentage of susceptible individuals in quarantine at any given time was small, we omitted this group from the model structure for simplicity. Students who tested positive and were subsequently isolated were removed from the testing pool for the next 90 days.

The OSU COVID-19 surveillance dataset consists of the dates of all tests for all students in the on-campus population, the outcomes of those tests, and the times individuals who tested positive entered isolation. Accordingly, with such data, we know the number of daily administered tests as well as daily test positive and negative rates. The number of daily tests at OSU along with the

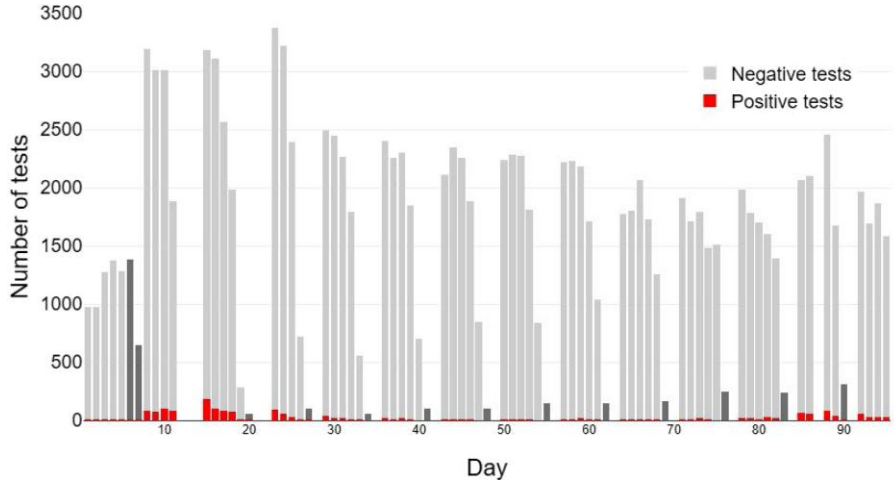

Figure 2. *Testing volume for SARS-CoV-2 at OSU.* This figure shows the daily number of tests administered to residential OSU students (18 years or older) starting from 17 August 2020 (Day 0). The bars are marked by testing result. Weekend testing volumes were typically lower (often zero on Sundays) and are shown in darker grey colour.

corresponding daily positive count is presented in Figure 2. As per institutional policy, we depict only data from 11,645 students who were at least 18 years old at the start of the testing regime. As we may see from the plot, at least for a portion of the time interval, the volume of daily testing on the first 4 days of the week appears reasonably similar across different weeks. The corresponding volume of testing in the later part of the week is seen to be considerably lower.

2.2 Disease transmission model

The framework of our statistical model is based on the classical Reed-Frost type SEIR model of an epidemic spread (see, for instance, Chapter 2 in Andersson and Britton (2012)). This model separates individuals in a population into four categories of susceptible (S), infected or exposed (E), infectious (I), and removed (R). The exposed are assumed to be infected but not yet infectious and the removed cannot be reinfected. We treat our population as closed, well mixed, and of known size. Below, we denote the initial susceptible population by n. Time is treated as a discrete, regular grid with units of days. We denote the counts of individuals in different categories (or compartments) at time t by S_t, E_t, I_t, and R_t and assume that they evolve according to the following rules.

- Each pair consisting of one individual from S_{t-1} and one from I_{t-1} has probability $\beta_t(n)$ of infectious contact, and each individual among S_{t-1} who experiences such a contact becomes infected/exposed starting at t.
- Following infection/exposure, a susceptible individual enters the exposed (E) compartment. Each individual i among E_{t-1} becomes infectious after τ_i days where $\tau_i \sim \text{Poisson}(\psi) + 1$.
- Each infectious individual i among I_{t-1} recovers after σ_i days, where $\sigma_i \sim \text{Poisson}(\gamma) + 1$.
- Each infectious individual i among I_{t-1} enters isolation at time r_i, where r_i is observed. We let $r_i = \infty$ for individuals who never test positive.
- Taken together, the previous two rules imply that each individual i among I_{t-1} enters the R compartment at time $\min\{\omega_i + \sigma_i, r_i\}$, where ω_i is the time individual i entered the I compartment.

Note that we add 1 to our Poisson random variables to ensure that individuals cannot instantly transition from S to I or from E to R. The choice to draw τ_i and σ_i from a Poisson distribution rather than the often-used Geometric distribution is motivated by the fact that such transition times are not in reality memoryless. The Poisson distribution concentrates these values around their population means, which may be more realistic. However, nothing about our model requires

that we use Poisson distributions, and one could other distributions as appropriate to the properties of the underlying disease.

The choice to draw τ_i and σ_i from a Poisson distribution rather than the often-used Geometric distribution also means that the usual count process (S_t, E_t, I_t, R_t) is no longer Markovian. In order to recover a Markovian process, we need information about individuals' sojourn times in E and I. In particular, the vector $(S_t, E_t, I_t, R_t, \tau, \sigma)$, where $\tau = \{\tau_i\}_{i=1}^n$ and $\sigma = \{\sigma_i\}_{i=1}^n$ describes a Markov process.

We assume that individuals in E are not yet detectable by RT-PCR testing as SARS-CoV-2 positive. By contrast, individuals in I are both infectious and detectable, though the detection probability may be less than 1. While the time from initial infection (exposure) to detectability varies across individuals, it is typically shorter than 5 days (Hart et al., 2022; He et al., 2020; Larremore et al., 2021), and the infectious period is typically around 10 days (CDC, 2023). Accordingly, we assume $\psi = 3$ and $\gamma = 10$ in our simulation study and data example.

Let Δ_t denote the daily decrease in the count of susceptibles. From the above discussion, we derive the following probability law for the daily increments of infection $\Delta_{t+1} = -(S_{t+1} - S_t)$ as follows:

$$\Delta_{t+1} \mid S_t, I_t, \beta_t(n), n \sim \text{Binomial}\left[S_t, 1 - (1 - \beta_t(n))^{I_t}\right]. \tag{1}$$

The model parameters of interest are the rate of infection transmission $\beta_t(n)$ and the initial conditions S_0, E_0, and I_0 $(R_0 = 0)$. An important feature of the model is that $\beta_t(n)$ depends on t and can potentially change at multiple time points. The model thus can accommodate behavioural changes over time, for example in response to perceived risk of infection, policy changes, weekend or holiday effects, and more.

Our model implicitly assumes a homogeneous mixing structure, with the underlying population network characterized by a complete graph. We make this choice for the sake of tractability rather than realism; certainly, the true underlying mixing structure is inhomogeneous. However, as demonstrated by the works of KhudaBukhsh et al. (2023, 2020) and Rempała (2023), both for DSA and more generally, the population dynamics arising from a variety of underlying mixing structures can often be approximated by a model with homogeneous mixing. We also acknowledge that observing mixing parameters can be challenging in many cases, such as the Ohio State student monitoring data. Despite attempts at Ohio State to use WiFi data for this purpose, the results were found to be ineffective for characterizing contact patterns (Banerji et al., 2023).

2.3 Survival and hazard functions

Our estimation approach builds on the DSA method developed by KhudaBukhsh et al. (2020). Specifically, we adapt the method to individual-level repeat testing data. There are several advantages of applying DSA to our setting such as the automatic correction for the interval censoring and the testing bias, both introduced by the data structure assumptions given in Section 2.1. See discussion in Section 3.1 for further details.

Consider the survival function $\mathcal{S}_t$ that describes the decay of susceptibles over time, along with its associated hazard function h_t. Let δ_i be the time that individual i experiences infectious contact and enters the E compartment, with the convention that $\delta_i = \infty$ if this never happens. Then $\mathcal{S}_t = P(\delta_i > t)$, the probability that an initially susceptible individual is still susceptible at time t. Define $\beta_t(n) = \beta_t/n$ when n is assumed to be large (i.e. we assume to have a large initial population of susceptibles). The probability that an initially susceptible individual stays susceptible until t is given by

$$\mathcal{S}_t = P(\delta_i > t) = \prod_{k=0}^{t-1}\left(1 - \frac{\beta_k}{n}\right)^{I_k}, \tag{2}$$

and thus the hazard function for a random susceptible being infected in $[t, t+1]$ is

$$h_{t+1} = \frac{\mathcal{S}_t - \mathcal{S}_{t+1}}{\mathcal{S}_t} = 1 - \frac{\mathcal{S}_{t+1}}{\mathcal{S}_t} = 1 - \left(1 - \frac{\beta_t}{n}\right)^{I_t}.$$

We note that for large n, $1-(1-\frac{\beta_t}{n})^{I_t} \approx \frac{\beta_t I_t}{n}$, which is the total rate of new infectious that appears in the mass action ODE form of this epidemic model.

As the E compartment is not observed (since individuals in E do not test positive), it is useful to consider the decay of the combined count of susceptible and exposed individuals. To this end, consider an initially susceptible individual. The probability that this individual has not yet entered I by time t can be computed by convolving over the transitions from S to E and E to I, giving

$$\widetilde{\mathcal{S}}_t = \sum_{k=1}^{t-1}\left(1-\left(1-\frac{\beta_k}{n}\right)^{I_k}\right)\mathcal{S}_{k-1}P(X>t-k)+\mathcal{S}_t,$$

where $X \sim \text{Poisson}[\psi]+1$.

2.4 Testing results and infection/exposure times

Since each on-campus student undergoes weekly SARS-CoV-2 testing, for each individual, we have available all test times and results. In particular, we know

- t_{neg}, the most recent time the individual was known to be susceptible or exposed, and
- t_{pos}, the first time the individual was known to be infectious.

Note that it is possible that a particular individual was infectious the first time they were observed, in which case we set $t_{neg}=0$. It is also possible that a particular individual has never been observed to be infectious, in which case we set $t_{pos}=\infty$.

We begin by considering the case where our test is perfectly sensitive and specific (we will later relax this assumption in Section 2.5. Given $\widetilde{\mathcal{S}}_t$, t_{neg}, and t_{pos}, we can find the probability that an individual became infectious on a particular day as follows:

- If $t_{neg}=i$ and $t_{pos}=j$, then for each $i<k\le j$, the probability that this individual became infectious on day k is $(\widetilde{\mathcal{S}}_{k-1}-\widetilde{\mathcal{S}}_k)/(\widetilde{\mathcal{S}}_i-\widetilde{\mathcal{S}}_j)$.
- If $t_{neg}=0$ and $t_{pos}=j$, then for each $0<k\le j$, the probability that this individual became infectious on day k is $(\widetilde{\mathcal{S}}_{k-1}-\widetilde{\mathcal{S}}_k)((1-\rho)-\widetilde{\mathcal{S}}_j)$, where $\rho=I_0/n$.
- If $t_{neg}=i$ and $t_{pos}=\infty$ and we have observed data until present time T, then for each $i<T$ the probability that this individual became infectious before time T is $\mathcal{P}_T:=(\widetilde{\mathcal{S}}_i-\widetilde{\mathcal{S}}_T)\widetilde{\mathcal{S}}_i$ and thus the probability this individual became infectious on day k with $i<k\le T$ is $\mathcal{P}_T(\widetilde{\mathcal{S}}_{k-1}-\widetilde{\mathcal{S}}_k)/(\widetilde{\mathcal{S}}_i-\widetilde{\mathcal{S}}_T)=(\widetilde{\mathcal{S}}_{k-1}-\widetilde{\mathcal{S}}_k)\widetilde{\mathcal{S}}_i$.

Of course, in practice tests are not perfect. However, we can adapt this idea of (imperfect) interval censoring to construct the distribution of ω_i, the time individual i enters the I compartment, given the collection of all individual test results.

2.5 Imperfect test sensitivity

The PCR tests used at OSU were highly specific, and so our main concern is imperfect sensitivity, that is, the possibility of false negative results. Recall that ω_i is the time individual i enters the I compartment (with the convention that $\omega_i=\infty$ if this never happens) and let D_i be the collection of test dates and corresponding results for individual i. Suppose that when applied to individual i, our test has known sensitivity $f_i(\cdot)$ that may depend on the time since individual i become infectious, which we call individual i's age of infection. Our goal is to characterize the distribution of δ_i given the survival function $\mathcal{S}_t$ and the data. We first observe that if we additionally knew τ_i and σ_i then

$$P(D_i \mid \omega_i, \tau_i, \sigma_i, f_i(\cdot), \mathcal{S}_t)$$

is straightforward to compute, since we know $f_i(\cdot)$ and individual i's age of infection at all times. We can then use Bayes Theorem to see that

$$P(\omega_i \mid D_i, \tau_i, \sigma_i, \beta, f_i(\cdot), \mathcal{S}_t) = \frac{P(D_i \mid \omega_i, \tau_i, \sigma_i, \beta, f_i(\cdot), \mathcal{S}_t) P(\omega_i \mid \tau_i, \mathcal{S}_t)}{\sum_{\omega_i} P(D_i \mid \omega_i, \tau_i, \sigma_i, \beta, f_i(\cdot), \mathcal{S}_t) P(\omega_i \mid \tau_i, \mathcal{S}_t)}. \tag{3}$$

Then in order to compute $P(\omega_i \mid D_i, \tau_i, \sigma_i, \beta, f_i(\cdot), \mathcal{S}_t)$ it remains only to compute $P(\omega_i \mid \tau_i, \mathcal{S}_t)$. We can note that since $\delta_i = \omega_i - \tau_i$, this is equivalent to computing $P(\delta_i \mid \mathcal{S}_t)$, which is simply given by the hazard function. In practice, we do not observe τ and σ. However, in our Bayesian estimation framework, we can use data augmentation to condition on them as part of our sampler.

It is possible that the sensitivity $f(\cdot)$ is not precisely known, and the results of fitting the model are sensitive to changes in $f(\cdot)$. In such cases, we recommend fitting the model for multiple choices of $f(\cdot)$ and incorporating the variation in results into the uncertainty quantification. Of course, changing $f(\cdot)$ will generally affect the results in a predictable way. Lower sensitivity will yield higher estimates of prevalence compared with the test positive rate and greater uncertainty about prevalence while higher sensitivity will yield lower estimates of prevalence compared with the test positive rate and less uncertainty about prevalence.

2.6 MCMC algorithm

We developed an iterated procedure implemented via a MH-within-Gibbs sampler algorithm to estimate the model parameters given the testing and removal data. Following initialization, we use the current prevalence estimate to compute the survival function (2). We then augment the data with the sojourn times in E and I, (τ, σ), and use this along with survival function and individual-level test results to propose daily incidence, which if accepted is then used to update the prevalence estimate. The detailed algorithm is as follows.

1. Initialize $\{\mathcal{S}_t\}_{t=1}^T$, $\{\beta_t\}_{t=1}^T$, ω, τ, σ.
2. Propose $(\omega', \tau', \sigma')$ by proposing each component independently as follows:
   (a) Propose $\tau_i' \sim \text{Poisson}(\psi) + 1$ for $i = 1, \ldots, n$ independently.
   (b) Propose $\sigma_i' \sim \text{Poisson}(\gamma) + 1$ for $i = 1, \ldots, n$ independently.
   (c) Propose $\omega_i' \sim P(\omega_i' \mid D_i, \tau_i, \sigma_i, \beta, f_i(\cdot)) = \frac{P(D_i \mid \omega_i, \tau_i, \sigma_i, \beta, f_i(\cdot)) P(\omega' \mid \beta, \mathcal{S})}{\sum_{\omega_i} P(D_i \mid \omega_i, \tau_i, \sigma_i, \beta, f_i(\cdot)) P(\omega' \mid \beta, \mathcal{S})}$, see (3).
3. Compute the derived quantities (S_t, E_t, I_t, R_t), δ_t, ϵ_t, Δ_t for $t = 1, \ldots, T$.
4. Compute the acceptance ratio

$$A = \frac{L(\omega', \tau', \sigma' \mid \beta, \mathcal{S}, f(\cdot)) g(\omega, \tau, \sigma \mid \beta, \mathcal{S}, f(\cdot))}{L(\omega, \tau, \sigma \mid \beta, \mathcal{S}, f(\cdot)) g(\omega', \tau', \sigma' \mid \beta, \mathcal{S}, f(\cdot))},$$

   where $L(\cdot)$ is the likelihood and $g(\cdot)$ is the proposal distribution. (See Section A for the full derivation of the acceptance ratio.)
5. Accept and set $(\omega, \tau, \sigma) = (\omega', \tau', \sigma')$ with probability $min(1, A)$.
6. Update β_t by drawing $\beta_t I_t / n \sim \text{Beta}(\Delta_t + a_t, S_{t-1} - \Delta_t + b_t)$ for $t = 1, \ldots, T$, where $\text{Beta}(a_t, b_t)$ is the prior on β_t.
7. Update $\mathcal{S}_t$ given $\{(\beta_t, I_t)\}_{t=1}^T$ using $\mathcal{S}_t = \mathcal{S}_0 \prod_{k=1}^t (1 - \frac{\beta_k}{n})^{I_k}$, see (2).
8. Go to step 2 and repeat until convergence.

This estimation scheme yields posterior samples for the survival function $\{\mathcal{S}_t\}_{t=1}^T$, the infection parameter $\{\beta_t\}_{t=1}^T$, the incidence ω, and the prevalence (as well as the other compartment counts) $\{(S_t, E_t, I_t, R_t)\}_{t=1}^T$. We update $\{\beta_t\}_{t=1}^T$ using a Beta-Binomial conjugate prior model, the incidence and prevalence counts via a MH step, and compute $\{\mathcal{S}_t\}_{t=1}^T$ using (2).

The main quantities of interest are the prevalence count and the transmission parameter β_t. Because the individual-level testing data is informative about the times that individuals entered the I compartment, we expect to produce precise estimates of prevalence. In addition to fully making use of this information, the advantage of our model is that it adjusts for both imperfect test

sensitivity and the effect of the repeated testing schedule in a principled way and allows for the estimation of transmission. We expect more uncertainty about the transmission parameter β_t, especially during periods when β_t is changing quickly with respect to the observed time.

We assume that ψ and γ, and $f_i(\cdot)$ are known. In principle, we could additionally estimate γ. However, under our assumptions in Section 2.1, infectious individuals typically move to R via isolation rather than natural recovery. Since the interval between tests is shorter than the expected recovery time, most individuals who become infectious will test at least once while infectious, and assuming a reasonably sensitive test, likely test positive and move to isolation before they naturally recover. Because of this, the particular choice of γ has only a small effect on the model dynamics, provided the choice is broadly reasonable. However, this also makes estimating γ difficult, as the observed data contains very little information about γ.

3 Results

3.1 Bias in naive, nonmechanistic modelling

Before we present the proposed IDSA model performance on data examples, let us first briefly discuss the alternative nonmechanistic approaches often considered in similar contexts in the statistical literature. Indeed, by now a plethora of approaches to analysing COVID-19 occurrences via count-regression models have been proposed (see, e.g. Chan et al., 2021; Kianifard & Gallo, 1995 and references therein). In our current setting of repeated testing, it is perhaps especially tempting to entertain a simpler and more intuitive alternative to IDSA, by modelling the epidemic using daily counts of tests administered and daily test positive rates. However, the sample of individuals tested each day is not random and depends on the specific testing regime. The daily test positive rate in the weekly testing scheme can be thought of as representative of the prevalence in the population eligible for testing on that day. However, the population ineligible for testing due to having already been tested that week has a smaller proportion of individuals in I because all those who were in I at the time of testing have since moved to R. Thus, the daily test positive rate overestimates the population prevalence except on the first day of each week. Some accounting for the interacting compartmental and testing processes is needed to obtain unbiased estimates of prevalence.

To give a simple example, we simulated 1,000 epidemic trajectories using similar settings as in Section 3.2 below. We assume perfect testing in this example in order to clearly illustrate our point; imperfect sensitivity biases the test positive rate downward compared with the prevalence and may make it difficult to observe the effects of the repeated testing schedule. We compare the naive estimate of prevalence computed using the formula (daily test positive rate $*(n - R_t)$) with the true value of I_t, and averaged over the 1,000 simulations. The results are presented in the right panel of Figure 3, illustrating a positive bias in the implied prevalence that increases with the true I_t and also over the course of the week (the duration of testing window). Indeed, note that for any day in the week-long testing window beyond day one ($d > 1$), the daily test positive rate has to overestimate the prevalence, since individuals in the tested sample will test positive so long as their infection time is smaller than d. Since an individual's test day is chosen uniformly at random from the days of the week, it is approximately independent of that individual's infection day so that the bias gets accumulated over the testing window. Admittedly, this heuristic ignores the effect of natural recoveries, but if the window between consecutive tests is shorter than the natural recovery time, which is an objective of the transmission control scheme (and is assumed in Section 3.3), then individuals who become infected and naturally recover between two consecutive scheduled tests will be rare.

In order to examine the implications of the bias of the test positive rate on the modelling strategy relying on daily incidence counts, the SEIR model and testing data were simulated (see Section 3.2 for details) giving us the hypothetical daily number of tests administered along with the daily test positive rate. Under the assumption that removals of infectious individuals are deterministic (occurring only at a fixed time after a positive test, and with no untested recoveries), we calculated the daily number of individuals in the S, E, or I compartments and fitted a Poisson generalized additive model to the simulated dataset. The model used the number of positive tests as the outcome variable, the log number of tests administered as the offset, and a penalized spline term for time via an adaptive spline basis (bs = 'ad') with otherwise default settings of the version

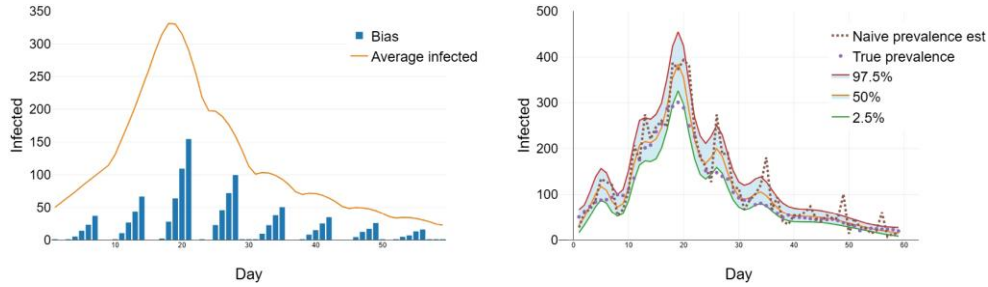

Figure 3. *Bias in testing-based estimates of prevalence. Left:* The bars depict average differences between daily estimates of prevalence computed from daily test positive rates and the true values of I_t (solid line) averaged over the 1,000 simulations. The bias is seen to increase in the course of the week and with true I_t. The mechanism of the bias is explained in Figure 1. *Right*: Poisson GAM fit (solid lines) of the prevalence along with the naive prevalence estimate (dotted line) obtained by $n*$(daily test positive rate) compared with the actual simulated counts (dots). The Poisson model is seen to severely overestimate I_t following the pattern of bias from the left panel. Although not shown here, similar results were also obtained using negative binomial regression model.

1.8–33 of R `mgcv` package function `gam()`. Prevalence estimates were then produced at each timepoint (day) by predicting the number of positive tests, if the entire nonremoved population had been tested (by setting the offset to the log number of nonremoved students). The results are shown in the right panel of Figure 3. As can clearly be seen from the plot, the Poisson model substantially overestimates the peak of the epidemic and exhibits large oscillations along the epidemic trajectory that are consistent with the accumulated bias in the naive prevalence estimates. We thus see the naive Poisson model is in fact attempting to fit (with some smoothing) these incorrect, overestimated prevalence values. Fitting a negative binomial model yielded similar results.

3.2 Simulation study

In order to assess the performance of the estimation algorithm proposed in Section 2.6, we performed a simulation study. We considered an SEIR epidemic in a population of size $n = 10{,}000$ over a period of $T = 98$ days (approximately one semester). In order to account for changing social behaviour and compliance with public health measures, we let β_t vary over the course of the epidemic, setting $\beta_t = .32$ for $t = 1, \ldots, 7$, $\beta_t = .40$ for $t = 8, \ldots, 14$, $\beta_t = 0.05$ for $t = 15, \ldots, 21$, $\beta_t = 0.10$ for $t = 22, \ldots, 56$, $\beta_t = .3$ for $t = 57, \ldots, 83$, and $\beta_t = .2$ for $t = 84, \ldots, 98$. We let $\psi = 3$ and $\gamma = 10$ so that individuals' sojourn times in E and I were Poisson(3) + 1 and Poisson(10) + 1 distributed respectively. We took the age of infection-dependent sensitivity for individual i $f_i(\cdot)$ to be a triangle starting at .8 at the start of the individual's infectious period, peaking at .9 30% of the way through the individual's infectious period, and decaying back to .8 at the end of the individual's infectious period. This is consistent with findings that viral loads for SARS-CoV-2 infections peak early in the infectious period (Larremore et al., 2021). The chosen magnitudes yield an 'average' sensitivity (the expected sensitivity of a test administered uniformly at random over the typical infectious period) consistent with sensitivity estimates in the meta-analysis of Butler-Laporte et al. (2021).

We assume that each individual in the population is tested weekly. We simulate this each week by numbering individuals $1, \ldots, 10{,}000$, permuting this sequence into a random order of individual tests distributed approximately uniformly over 7 days, Monday through Sunday. Individuals who test positive are moved to isolation (removed and sent to the R compartment) 2 days after being tested to model the delay in test outcomes reporting. Individuals may enter the R compartment via natural recovery or isolation. However, because the typical test interval is shorter than the typical infection length, most individuals who enter the R compartment will do so via isolation.

We chose these settings for our simulation study because they produced an epidemic curve qualitatively similar to the one observed among on-campus students during the Autumn 2020 semester at The OSU and are broadly consistent with what is known about ancestral SARS-CoV-2, which was the dominant strain at that time. The epidemic has a peak during the third week of the semester followed by an extended period of low prevalence and then a second, smaller peak that begins to decay at the end of the semester.

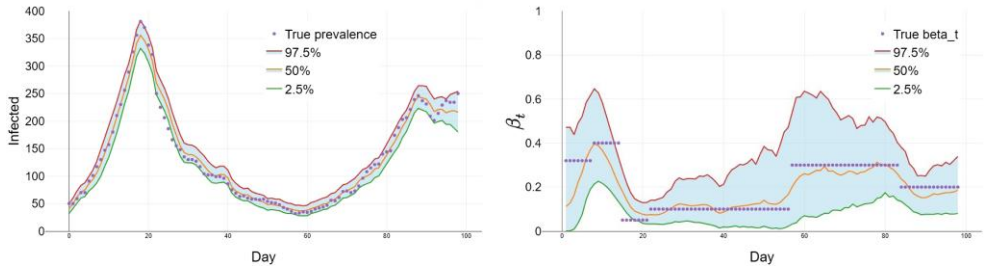

Figure 4. *IDSA simulation study model fit over a 98-day period (chosen to match the timescale of the OSU data). Left:* The model estimates of the prevalence represented by the posterior quantile plots (smooth curves) compared with the true value from the simulated trajectory. *Right:* Model-based posterior estimates of β_t compared with the true values used to generate the simulated data.

For each individual, we recorded the times and results of all tests as well as the time the individual was sent to isolation if that occurred. For comparison, we also record the true numbers of S, E, I, and R individuals each day. These numbers are not used to fit the model but rather to assess the quality of model fit. We fit the model using the algorithm in Section 2.6. We took the prior on β_t as Beta(.5, $.5/\beta_{t-1}$) to be weakly informative and centred on β_{t-1}, although in practice, we found that the results are not much different if we instead use the noninformative prior Beta(1, 1) or the Jeffries prior Beta(.5, .5).

When running the MCMC, we proposed $(\omega_i', \tau_i', \sigma_i')$ for only 10% of individuals in Step 2 on each iteration, which we found was helpful for obtaining a reasonable acceptance rate for our Metropolis step in 5. We ran the MCMC for 15,000 iterations, observing an acceptance rate of 48.5%. We discarded the first 5,000 samples as burn-in and thinned the remaining 10,000 sample by a factor of 10, resulting in 1,000 posterior samples. MCMC diagnostics suggested no concerns with the mixing or convergence of the chain, and a representative sample of MCMC trace plots is given in Appendix B.

The results of the IDSA fit to the simulated data are presented in the two panels of Figure 4. In the left panel, we plotted prevalence I_t, along with its 2.5%, median, and 97.5% posterior quantiles over the time horizon of $T = 98$ days. The comparison of I_t with the median model prediction indicates a good fit, and the model correctly identifies the timing and size of the epidemic peaks. The 95% posterior interval covers 94.9% of the true values of I_t. Notably, our model also shows no evidence of systematically overestimating the prevalence due to the repeat testing regime. The uncertainty of our prevalence estimates is low, which we expect given that using the complete testing history of all individuals in the IDSA framework is highly informative about the prevalence. The uncertainty increases toward the end of the period because of the backfilling problem. That is, at the end of the period, there are infectious individuals whose next (likely positive) test is still in the future, and the model fit tends towards the expected continuation of the epidemic without knowing the results of these tests.

The left panel of Figure 4 shows the true value of β_t against the 2.5%, median, and 97.5% posterior quantiles of β_t. The uncertainty associated with our estimates of β_t is larger, particularly at the beginning of the time period when there is not yet much information about transmission. However, we see that our estimates of β_t correctly identify the trend even when β_t is changing rapidly, and the posterior median provides a good estimate of β_t during periods when the true value of β_t is stable.

The code used to perform the simulation study and generate the figures can be found at https://github.com/mwwascher/IDSA.

3.3 Analysis of OSU COVID-19 surveillance data

In this section, we present the data analysis that has motivated the IDSA model. We use the slightly altered[1] surveillance dataset on student testing results collected by The OSU between 17 August and 24 November 2020 as part of the university's plan to manage and mitigate COVID-19 during

[1] Students who were minors were removed from our analysis as per institutional policy.

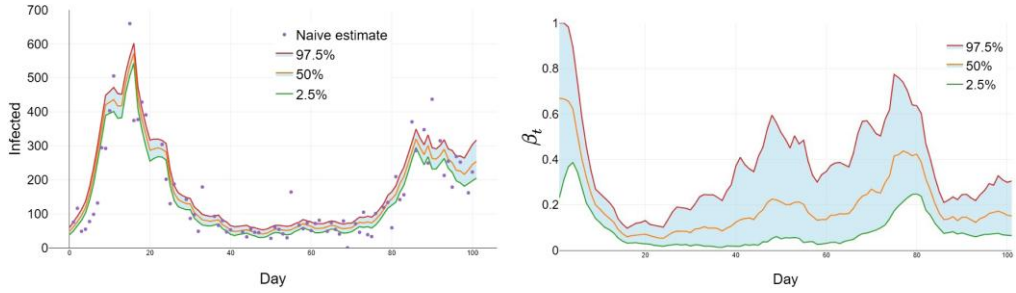

Figure 5. *IDSA model fit to OSU COVID-19 data. Left:* The model estimates of prevalence (lines within the 95% credibility envelope) versus $n \times$ daily test positive rate on days with at least 100 tests administered. *Right:* Model-based posterior estimate of the transmission parameter β_t. The median and 2.5% and 97.5% quantiles of the posterior estimates are plotted as smooth solid curves within the 95% region of credibility. Because we assume testing is imperfect, the test positive rate is an underestimate of the true prevalence among those tested each day, and we do not necessarily expect the test positive rate to fall above the model estimates, even in the presence of upward bias due to the testing scheme.

the Autumn semester 2020 with students on campus. The OSU's internal policy was to weekly test each of $n = 12{,}567$ students living on campus. In the event of a positive test, the student was isolated for 10 days and contact tracing was initiated. We observed that in most cases, there was a 2-day delay between administering the test and quarantining positive testing students. Students who tested positive were subsequently quarantined and removed from the testing pool for 90 days.

The OSU dataset consists of the dates and results of all test for each individual, as well as the time each individual entered isolation, if that occurred. From this data, we can also compute the total number of tests administered each day and the daily number of positive and negative tests.

We fit the IDSA model to the data by applying the MH-within-Gibbs sampler algorithm described in Section 2.6. As in our simulation study, we let $\psi = 3$ and $\gamma = 10$ so that individuals' sojourn times in E and I were Poisson(3) + 1 and Poisson(10) + 1 distributed, respectively. We took the age of infection-dependent sensitivity for individual i, $f_i(\cdot)$, to be a triangle starting at .8 at the start of the individual's infectious period, peaking at .9 30% of the way through the individual's infectious period, and decaying back to .8 at the end of the individual's infectious period.

We took the prior on β_t as Beta(.5, $.5/\beta_{t-1}$) to be weakly informative and centred on β_{t-1}. When running the MCMC, we updated $(\omega_i, \tau_i, \sigma_i)$ for 1,000 (out of 11,645) individuals selected uniformly at random on each iteration, which we found helpful for obtaining a reasonable acceptance rate for the Metropolis step in 5. of our MCMC algorithm in Section 2.6. We ran the MCMC for 15,000 iterations, observing an acceptance rate of 50.0%. We discarded the first 5,000 samples as burn-in and thinned the remaining 10,000 samples by a factor of 10, resulting in 1,000 posterior samples. See trace plots in Figure A1 in the Appendix.

The results of the IDSA fit to the OSU data are presented in the two panels of Figure 5. In the left panel, we plotted the 2.5%, median, and 97.5% posterior quantiles of the 5-day moving average of estimated prevalence against the observed test positive rate on days with at least 100 tests administered. We see that the estimated prevalence matches the general shape of the test positive rate. The true prevalence is unknown.

The observed test positive rate may differ from the true prevalence due to sampling error, imperfect testing, and bias from the repeated testing schedule, so we do not expect that posterior estimates necessarily cover the observed test positive rate values. In fact, we see that sampling error can be substantial, and the test positive rate sometimes exhibits large oscillations over a short time period (on days with relatively fewer tests). The IDSA prevalence estimates do not exhibit such large oscillations because IDSA uses the longitudinal information in the testing data. Because imperfect testing creates a downward bias and the repeated test schedule creates an upward bias, it is not obvious whether we should expect the test positive rate to be systematically higher or lower than the true prevalence in this case.

The right panel of Figure 5 shows 2.5%, median, and 97.5% posterior quantiles of the transmission parameter β_t. We observe that transmission is high early in the semester, consistent with a large peak in test positive rate and estimated prevalence, which is followed by an extended

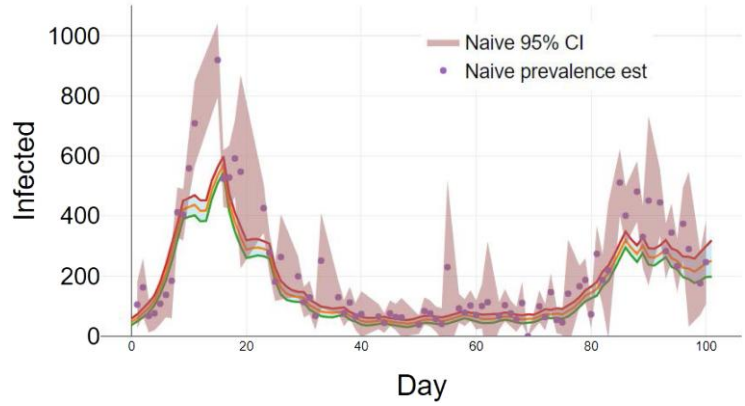

Figure 6. *Comparison of IDSA model fit to OSU COVID-19 data to a naive estimation method applied to this same data:* The dots give pointwise daily prevalence estimates obtained from the usual Binomial MLE, and the associated solid band gives the pointwise 95% confidence intervals for these estimates. The solid lines defining the 95% credibility envelop are the IDSA estimates, as before. The naive estimates tend to be larger and have greater uncertainty compared with the IDSA estimates, particularly when prevalence is high. They are also not age-of-infection sensitivity-adjusted; therefore, they differ from those in the left panel of Figure 5. Refer to the text for details.

period of low to moderate transmission. The transmission parameter rises again toward the end of the semester where we see a second smaller peak in test positive rate and estimated prevalence.

Figure 6 compares the IDSA model estimates on the OSU data to a naive estimation method that obtains pointwise estimates and confidence intervals from the usual Binomial MLEs and associated 95% confidence interval on this data. To compute the Binomial MLEs and associated confidence intervals adjusted for imperfect testing, we use the 'average' sensitivity (the expected sensitivity of a test administered uniformly at random over the typical infectious period) denoted by f and γ (as the naive method does not allow for dependence on age-of-infection). As expected given our heuristic and results in Section 3.1, we observe that the naive estimates tend to be larger and have greater uncertainty than the IDSA estimates, especially when prevalence is high.

4 Discussion and conclusions

There has been an exponential growth in the volume of mathematical epidemic modelling literature since the start of the COVID-19 pandemic. However, few researchers have concentrated on rigorous statistical models that consider repeat testing in closed populations, such as student communities on college campuses, as we have in our study. This issue was particularly pertinent in the early stages of the pandemic. Here, we discuss some recent works that are relevant and to some extent comparable to ours. In Chang et al. (2020), the authors built a fairly detailed model based on Kaplan (2020) accounting for important considerations such as test frequency, test specificity, and dependence of test sensitivity on time since infection. The authors of Paltiel et al. (2020) considered an extended discrete-time SEIR compartmental model for a hypothetical cohort of 5,000 students to suggest that frequent screening (every 2 days) of all students might be required to control outbreaks. Both Chang et al. (2020) and Paltiel et al. (2020) share some similarities with our work. The crucial differences are in the model description (ours appears to be simpler) and statistical methodology employed to estimate the model parameters. While Paltiel et al. (2020) is primarily a simulation-based study, Chang et al. (2020) borrows a number of parameter values from the literature. Another simulation-based work is Rennert et al. (2020), where the authors use an extended SEIR model to assess the role of presemester screening in averting early and large surges of COVID-19 infections. An advantage of works such as Rennert et al. (2020) is that they could be used to test potential intervention strategies in more realistic settings compared with traditional mass-action deterministic models. In a similar vein, the authors of Arnst et al. (2022) develop a MCMC-based Bayesian method to estimate a subset of parameters of a hybrid stochastic model for transmission of COVID-19 on the University of Liège campus. The starting point of their model development is a massive system of ordinary differential equations, which is typical of compartmental modelling approaches. In order to derive a likelihood function, they construct a

corresponding continuous time Markov chain model, which can be approximated by a diffusion process in the limit of a large population. This is indeed a principled approach to parameter inference, notwithstanding the issues related to unidentifiable parameters, which they assume known from various sources.

In a recent article, Muller and Muller (2021) developed an SEIR-type compartmental model to study the spread of COVID-19 on a university campus among a homogeneously mixing population. They validate their model by fitting it to the data available from Villanova University's COVID Dashboard for the Autumn 2020 semester. The difference between their work and ours is that they like Arnst et al. (2022) borrow the majority of their parameters from the literature. In a retrospective study Rennert et al. (2021), the authors considered a meta-population model using a cross-coupling matrix for SARS-CoV-2 transmission to evaluate testing strategies implemented by Clemson University. A similar study for the Cornell University is Frazier et al. (2022), where the authors fit the parameters by minimizing squared errors. As opposed to mass-action models, the authors of Hill et al. (2021) built an elaborate network-based model with four layers (corresponding to households, study groups, societies, and social contacts) and used a combination of a maximum likelihood-based and literature-borrowed estimates to fit an SEIR-type model to study the transmission of COVID-19 in the UK university setting. A similar study is done in Enright et al. (2021). While population models require fewer parameters, agent-based models are often preferred because of their ability to capture realistic dynamics. Such an agent-based model was considered for instance in Cator et al. (2022). Although our approach is based on individual-level data, our model does not use an individual-level likelihood, like for instance in Bridgen et al. (2024) and Pokharel and Deardon (2022), but rather approximates it with the aggregated quantity, akin to the idea of the propagation of chaos in stochastic dynamical systems (see Cappelletti & Rempala, 2023).

An alternative approach to assessing potential infection risks involves collecting data on SARS-CoV-2 viral load from air and surface samples, as demonstrated by Zhang et al. (2022). Despite contextual and scientific similarities, findings in these articles may not generalize to other diseases and institutions due to variations in disease transmission models and parameters, especially those derived from diverse literature sources. Consequently, the imperative for a statistical method persists, one built upon a simple disease transmission model that reliably estimates parameters from repeated testing data.

Presented here is a statistical IDSA model providing estimates for prevalence count and transmission rate. The model, showcased in Section 3, demonstrates promising fits in both synthetic data examples and the analysis of OSU repeated testing data. The IDSA model's flexibility in capturing changing epidemic patterns is attributed to allowing the key transmission parameter β_t to vary with time and accounting for age-of-infection-dependent sensitivity. While fully identifiable, the model requires a sufficiently high volume of daily and weekly data for accurate fitting, as exemplified by the OSU dataset, where each week of repeated testing contributed approximately 12,000 new data points for parameter estimation. Although not detailed in this discussion, our experience with the IDSA model applied to the OSU dataset indicates favourable agreement between model forward predictions and actual data, mitigating concerns related to overfitting in complex mechanistic models.

The analysis of the OSU dataset presented in this article represents one of the few comprehensive statistical studies of repeated SARS-CoV-2 testing data among a large population of US college undergraduates. For the OSU dataset, we assumed an approximately closed population, informed by evidence from the monitoring of wifi data (see Banerji et al., 2023), and disregarded the importation of infection from outside of campus. Therefore caution should be exercised in interpreting our transmission estimates for OSU in temporal regions of low prevalence. For instance, a consistent low-level importation of cases could lead to $\beta_t > 0$, despite minimal transmission within the residential undergraduate community. For the sake of actual campus predictions in 2020 Autumn semester, we expanded the model to include a constant baseline level of positive tests per day to account for this. This baseline level may correspond to false positives, externally imported infections, or a combination of the two. Distinguishing between false positives and imported infections among these baseline positives may require additional data and is closely tied to quantifying the significance of transmission between residential and off-campus members of the university community. We plan to explore this issue further in future work, employing a multi-population DSA model.

We note that with an increasing amount of residential surveillance data becoming available, further extensions of the IDSA model beyond multi-populations are also possible.

However, even though such more general models may have the ability to adjust for different types of interactions and social mixing *between* groups, they still may not properly account for the social networks of contacts *within* different groups. Thus, additional work is needed for examining SARS-CoV-2 dynamics in relevant on- and off-campus populations, in order to further improve the accuracy of the IDSA model-based predictions. This is also left for future investigation as part of the expansion of the framework presented here. Despite these limitations, we anticipate that the presented framework will prove valuable both in a general sense and specifically in the context of introducing and assessing various intervention types, including different vaccination schemes for residents. This aligns with policy suggestions offered by the modelling community, such as those by Wang et al. (2021), at the initial rollout of the SARS-CoV-2 vaccines.

Acknowledgments

W.R.K.B. was supported by an International Collaboration Fund awarded by the Faculty of Science, University of Nottingham (UoN). G.A.R. and M.W. were supported by the US National Science Foundation (NSF-DMS # 2027001). G.A.R. was also supported by the HEALMOD initiative at The Ohio State University.

Conflict of interest: None declared.

Author contributions

M.B.Q. conceived the framework for data collection. M.W., P.M.S., W.R.K.B., J.T., and G.A.R. developed the statistical model. M.W. analysed the results and performed numerical simulations. M.W., G.A.R., and W.R.K.B. wrote the manuscript. All authors reviewed and approved the manuscript.

Data availability

The human data collection and analysis was approved under The Ohio State University IRB protocol 2021H0189. The anonymized dataset and computer code used to generate figures and analyse data are available from https://github.com/mwwascher/IDSA.

Appendix A. Derivation of the MH acceptance ratio

The acceptance ratio for $(\omega', \tau', \sigma')$ in step 4. of our estimation procedure in Section 2.6 is given by

$$A = \frac{L(\omega', \tau', \sigma' \,|\, \beta, \mathcal{S}_t, f(\cdot))g(\omega, \tau, \sigma \,|\, \beta, \mathcal{S}_t, f(\cdot))}{L(\omega, \tau, \sigma \,|\, \beta, \mathcal{S}_t, f(\cdot))g(\omega', \tau', \sigma' \,|\, \beta, \mathcal{S}_t, f(\cdot))},$$

where $L(\omega, \tau, \sigma \,|\, \beta, \mathcal{S}, f(\cdot))$ is the likelihood and $g(\omega, \tau, \sigma \,|\, \beta, \mathcal{S}_t, f(\cdot))$ is the proposal distribution. We can compute

$$\begin{aligned} L(\omega, \tau, \sigma \,|\, \beta, \mathcal{S}_t, f(\cdot)) = &\left(\prod_{t=1}^{T}\left[1-(1-\frac{\beta_t}{n})^{I_t}\right]^{\Delta_t}\left[(1-\frac{\beta_t}{n})^{I_t}\right]^{\mathcal{S}_t-\Delta_t}\right) \\ &\times\left(\prod_{i=1}^{n} f_\tau(\tau_i)\right)\left(\prod_{i=1}^{n} f_\sigma(\sigma_i)\right)\left(\prod_{i=1}^{n} P(D_i \,|\, \omega_i, \tau_i, \sigma_i, \beta, \mathcal{S}_t, f_i(\cdot))\right), \end{aligned}$$

and we use the proposal distribution

$$g(\omega, \tau, \sigma \,|\, \beta, \mathcal{S}, f(\cdot)) = \left(\prod_{i=1}^{n} f_\tau(\tau_i)\right)\left(\prod_{i=1}^{n} f_\sigma(\sigma_i)\right)\left(\prod_{i=1}^{n} \frac{P(D_i \,|\, \omega_i, \tau_i, \sigma_i, \beta, \mathcal{S}, f_i(\cdot))P(\omega_i \,|\, \tau_i, \mathcal{S}_t)}{\sum_{\omega_i} P(D_i \,|\, \omega_i, \tau_i, \sigma_i, \beta, \mathcal{S}, f_i(\cdot))P(\omega_i \,|\, \tau_i, \mathcal{S}_t)}\right).$$

Note that $P(\omega_i \,|\, \tau_i, \mathcal{S}_t)$ is the hazard at time $\omega_i - \tau_i$, $h_{\omega_i-\tau_i}$, and $\frac{P(D_i \,|\, \omega_i, \tau_i, \sigma_i, \beta, \mathcal{S}, f_i(\cdot))P(\omega_i \,|\, \tau_i, \mathcal{S}_t)}{\sum_{\omega_i} P(D_i \,|\, \omega_i, \tau_i, \sigma_i, \beta, \mathcal{S}, f_i(\cdot))P(\omega_i \,|\, \tau_i, \mathcal{S}_t)}$ is the conditional probability $P(\omega_i \,|\, D_i, \tau_i, \sigma_i, \beta, \mathcal{S}_t, f_i(\cdot))$ obtained using Bayes rule in equation 3. After

some cancellation and rearranging, we see that

$$
\begin{aligned}
A &= \frac{L(\omega', \tau', \sigma' \mid \beta, \mathcal{S}_t, f(\cdot))g(\omega, \tau, \sigma \mid \beta, \mathcal{S}_t, f(\cdot))}{L(\omega, \tau, \sigma \mid \beta, \mathcal{S}_t, f(\cdot))g(\omega', \tau', \sigma' \mid \beta, \mathcal{S}_t, f(\cdot))} \\
&= \left\{ \left(\prod_{t=1}^{T} \left[1 - (1 - \frac{\beta_t}{n})^{I'_t} \right]^{\Delta'_t} \left[(1 - \frac{\beta_t}{n})^{I'_t} \right]^{S'_t - \Delta'_t} \right) \left(\prod_{i=1}^{n} P(D_i \mid \omega'_i, \tau'_i, \sigma'_i, \beta, \mathcal{S}_t, f_i(\cdot)) \right) \right. \\
&\quad \left. \times \left(\prod_{i=1}^{n} \frac{P(D_i \mid \omega_i, \tau_i, \sigma_i, \beta, \mathcal{S}_t, f_i(\cdot))P(\omega_i \mid \tau_i, \mathcal{S}_t)}{\sum_{\omega_i} P(D_i \mid \omega_i, \tau_i, \sigma_i, \beta, \mathcal{S}_t, f_i(\cdot))P(\omega_i \mid \tau_i, \mathcal{S}_t)} \right) \right\} \\
&\quad \Big/ \left\{ \left(\prod_{t=1}^{T} \left[1 - (1 - \frac{\beta_t}{n})^{I_t} \right]^{\Delta_t} \left[(1 - \frac{\beta_t}{n})^{I_t} \right]^{S_t - \Delta_t} \right) \left(\prod_{i=1}^{n} P(D_i \mid \omega_i, \tau_i, \sigma_i, \beta, \mathcal{S}_t, f_i(\cdot)) \right) \right. \\
&\quad \left. \times \left(\prod_{i=1}^{n} \frac{P(D_i \mid \omega'_i, \tau'_i, \sigma'_i, \beta, \mathcal{S}_t, f_i(\cdot))P(\omega_i \mid \tau_i, \mathcal{S}_t)}{\sum_{\omega'_i} P(D_i \mid \omega'_i, \tau'_i, \sigma'_i, \beta, \mathcal{S}_t, f_i(\cdot))P(\omega_i \mid \tau_i, \mathcal{S}_t)} \right) \right\} \\
&= \frac{\left(\prod_{t=1}^{T} \left[1 - (1 - \frac{\beta_t}{n})^{I'_t} \right]^{\Delta'_t} \left[(1 - \frac{\beta_t}{n})^{I'_t} \right]^{S'_t - \Delta'_t} \right) \left(\prod_{i=1}^{n} \sum_{\omega'_i} P(D_i \mid \omega'_i, \tau'_i, \sigma'_i, \beta, \mathcal{S}_t, f_i(\cdot))P(\omega_i \mid \tau_i, \mathcal{S}_t) \right)}{\left(\prod_{t=1}^{T} \left[1 - (1 - \frac{\beta_t}{n})^{I_t} \right]^{\Delta_t} \left[(1 - \frac{\beta_t}{n})^{I_t} \right]^{S_t - \Delta_t} \right) \left(\prod_{i=1}^{n} \sum_{\omega_i} P(D_i \mid \omega_i, \tau_i, \sigma_i, \beta, \mathcal{S}_t, f_i(\cdot))P(\omega_i \mid \tau_i, \mathcal{S}_t) \right)}.
\end{aligned}
$$

Appendix B. MCMC trace plots

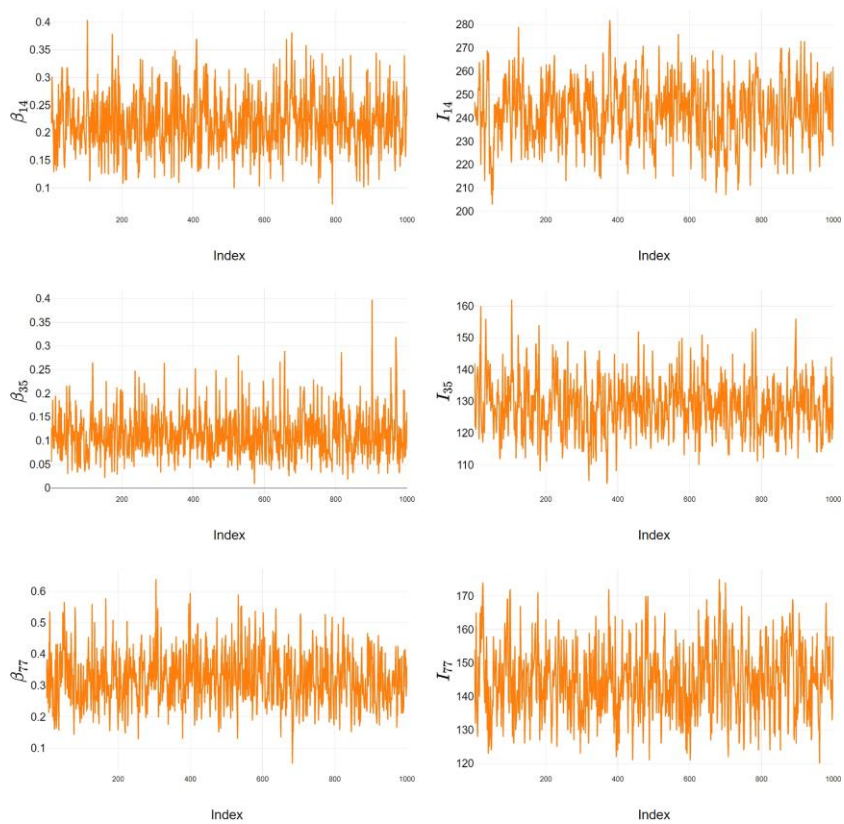

Figure A1. Representative MCMC trace plots for the posteriors of β_t and I_t for $t = \{14, 35, 77\}$. Overall, the diagnostic trace plots suggest good mixing and convergence properties of the chain, as well as no undue correlations among posterior parameters (plots not shown).

Appendix C. Summary of notation

Table A1. Summary of notation

Symbol	Description
S_t	Count of susceptible individuals at time t
E_t	Count of exposed individuals at time t
I_t	Count of infectious individuals at time t
R_t	Count of removed individuals at time t
Δ_t	The count of individuals who move from S to E from day $t-1$ to day t
β_t	Infection rate parameter at time t
ψ	Parameter governing sojourn times in E
γ	Parameter governing sojourn times in I
δ_i	The time at which individual i experiences infectious contact and enters the E compartment
ω_i	The time at which individual i enters the I compartment
τ_i	Individual i's sojourn time in E
σ_i	Individual i's sojourn time in I
D_i	The collection of test dates and results for individual i
$f_i(\cdot)$	Individual i's (potentially age-of-infection-dependent) test sensitivity
$\mathcal{S}_t$	Probability an initially susceptible individual is still susceptible at time t
$\widetilde{\mathcal{S}}_t$	Probability an initially noninfectious individual has not become infectious by time t

References

Andersson H., & Britton T. (2012). *Stochastic epidemic models and their statistical analysis*. (Vol. *151*). Springer Science & Business Media.

Arnst M., Louppe G., Van Hulle R., Gillet L., Bureau F., & Denoël V. (2022). A hybrid stochastic model and its Bayesian identification for infectious disease screening in a university campus with application to massive COVID-19 screening at the University of Liège. *Mathematical Biosciences*, *347*, 108805. ISSN 0025-5564. https://www.sciencedirect.com/science/article/pii/S0025556422000219. https://doi.org/10.1016/j.mbs.2022.108805

Banerji N., Chang S., Perrault A., Berger-Wolf T. Y., & Quam M. (2023). Pandemic data collection, management, analysis and decision support: A large urban university retrospective. https://openreview.net/pdf?id=BNU_N-7EIR.

Bridgen J. R., Lewis J. M., Todd S., Taegtmeyer M., Read J. M., & Jewell C. P. (2024). A Bayesian approach to identifying the role of hospital structure and staff interactions in nosocomial transmission of SARS-CoV-2. *Journal of The Royal Society Interface*, *21*(212), 20230525. https://doi.org/10.1098/rsif.2023.0525

Butler-Laporte G., Lawandi A., Schiller I., Yao M., Dendukuri N., McDonald E. G., & Lee T. C. (2021, March). Comparison of saliva and nasopharyngeal swab nucleic acid amplification testing for detection of SARS-CoV-2: A systematic review and meta-analysis. *JAMA Internal Medicine*, *181*(3), 353–360. ISSN 2168-6106. https://doi.org/10.1001/jamainternmed.2020.8876

Cappelletti D., & Rempala G. A. (2023, June). Individual molecules dynamics in reaction network models. *SIAM Journal on Applied Dynamical Systems*, *22*(2), 1344–1382. ISSN 1536-0040. https://doi.org/10.1137/21M1459563

Cator D., Huang Q., Mondal A., Ndeffo-Mbah M., & Gurarie D. (2022). Individual-based modeling of COVID-19 transmission in college communities. *Mathematical Biosciences and Engineering*, *19*(12), 13861–13877. https://doi.org/10.3934/mbe.2022646

CDC (2023). Ending isolation and precautions for people with COVID-19: Interim guidance. https://www.cdc.gov/coronavirus/2019-ncov/hcp/duration-isolation.html.

Chan S., Chu J., Zhang Y., & Nadarajah S. (2021). Count regression models for COVID-19. *Physica A: Statistical Mechanics and its Applications*, *563*, 125460. https://doi.org/10.1016/j.physa.2020.125460

Chang J. T., Crawford F. W., & Kaplan E. H. (2020). Repeat SARS-CoV-2 testing models for residential college populations. *Health Care Management Science*, *0*, 1–14. http://doi.org/10.1007/s10729-020-09526-0

Enright J., Hill E. M., Stage H. B., Bolton K. J., Nixon E. J., Fairbanks E. L., Tang M. L., Brooks-Pollock E., Dyson L., Budd C. J., Hoyle R. B., Schewe L., Gog J. R., & Tildesley M. J. (2021). SARS-CoV-2 infection in UK

university students: Lessons from September–December 2020 and modelling insights for future student return. *Royal Society Open Science*, *8*(8), 210310. https://doi.org/10.1098/rsos.210310

Frazier P. I., Cashore J. M., Duan N., Henderson S. G., Janmohamed A., Liu B., Shmoys D. B., Wan J., & Zhang Y. (2022). Modeling for COVID-19 college reopening decisions: Cornell, a case study. *Proceedings of the National Academy of Sciences*, *119*(2), e2112532119. https://doi.org/10.1073/pnas.2112532119

Gressman P. T., & Peck J. R. (2020). Simulating COVID-19 in a university environment. *Mathematical Biosciences*, *328*, 108436. https://doi.org/10.1016/j.mbs.2020.108436

Hart W. S., Miller E., Andrews N. J., Waight P., Maini P. K., Funk S., & Thompson R. N. (2022). Generation time of the alpha and delta SARS-CoV-2 variants: An epidemiological analysis. *The Lancet Infectious Diseases*, *22*(5), 603–610. https://doi.org/10.1016/S1473-3099(22)00001-9

He X., Lau E. H. Y., Wu P., Deng X., Wang J., Hao X., Lau Y. C., Wong J. Y., Guan Y., Tan X., Mo X., Chen Y., Liao B., Chen W., Hu F., Zhang Q., Zhong M., Wu Y., Zhao L., …Leung G. M. (2020). Temporal dynamics in viral shedding and transmissibility of COVID-19. *Nature Medicine*, *26*(5), 672–675. https://doi.org/10.1038/s41591-020-0869-5

Hill E. M., Atkins B. D., Keeling M. J., Tildesley M. J., & Dyson L. (2021). Modelling SARS-CoV-2 transmission in a UK university setting. *Epidemics*, *36*, 100476. ISSN 1755-4365. https://www.sciencedirect.com/science/article/pii/S175543652100030X. https://doi.org/10.1016/j.epidem.2021.100476

Kahanec M., Lafférs L., & Schmidpeter B. (2021). The impact of repeated mass antigen testing for COVID-19 on the prevalence of the disease. *Journal of Population Economics*, *34*(4), 1105–1140. https://doi.org/10.1007/s00148-021-00856-z

Kaplan E. H. (2020). Containing 2019-nCoV (Wuhan) coronavirus. *Health Care Management Science*, *23*(3), 311–314. https://doi.org/10.1007/s10729-020-09504-6

KhudaBukhsh W. R., Bastian C. D., Wascher M., Klaus C., Sahai S. Y., Weir M. H., Kenah E., Root E., Tien J. H., & Rempała G. A. (2023). Projecting COVID-19 cases and hospital burden in Ohio. *Journal of Theoretical Biology*, *561*, 111404. ISSN 0022-5193. https://www.sciencedirect.com/science/article/pii/S0022519322003952. https://doi.org/10.1016/j.jtbi.2022.111404

KhudaBukhsh W. R., Choi B., Kenah E., & Rempała G. A. (2020). Survival dynamical systems: Individual-level survival analysis from population-level epidemic models. *Interface Focus*, *10*(1), 20190048. https://doi.org/10.1098/rsfs.2019.0048

Kianifard F., & Gallo P. P. (1995). Poisson regression analysis in clinical research. *Journal of Biopharmaceutical Statistics*, *5*(1), 115–129. https://doi.org/10.1080/10543409508835101

Larremore D. B., Wilder B., Lester E., Shehata S., Burke J. M., Hay J. A., Tambe M., Mina M. J., & Parker R. (2021). Test sensitivity is secondary to frequency and turnaround time for COVID-19 screening. *Science Advances*, *7*(1), eabd5393. https://doi.org/10.1126/sciadv.abd5393

Maloney J. (2021). A first look at the 2020-21 NBA COVID protocols, including how long players who test positive will have to sit. *CBS.COM*, https://tinyurl.com/y44cr9yb: Date accessed January 2021.

McCabe R., & Donnelly C. A. (2021). Disease transmission and control modelling at the science–policy interface. *Interface Focus*, *11*(6), 20210013. https://doi.org/10.1098/rsfs.2021.0013

Muller K., & Muller P. A. (2021). Mathematical modelling of the spread of COVID-19 on a university campus. *Infectious Disease Modelling*, *6*, 1025–1045. ISSN 2468-0427. https://doi.org/10.1016/j.idm.2021.08.004

OSU Monitoring Team. (2021). Safe and Healthy Buckeyes. The Ohio State University COVID-19 Dashboard, https://safeandhealthy.osu.edu/dashboard. Date accessed April, 2024.

Paltiel A. D., Zheng A., & Walensky R. P. (2020). Assessment of SARS-CoV-2 screening strategies to permit the safe reopening of college campuses in the United States. *JAMA Network Open*, *3*(7), e2016818–e2016818. https://doi.org/10.1001/jamanetworkopen.2020.16818

Panovska-Griffiths J., Kerr C., Stuart R. M., Mistry D., Klein D., Viner R. M., & Bonell C. (2020). Determining the optimal strategy for reopening schools, work and society in the UK: Balancing earlier opening and the impact of test and trace strategies with the risk of occurrence of a secondary COVID-19 pandemic wave. *The Lancet Child & Adolescent Health*, *4*, 11817–827. https://doi.org/10.1016/S2352-4642(20)30250-9

Pokharel G., & Deardon R. (2022). Emulation-based inference for spatial infectious disease transmission models incorporating event time uncertainty. *Scandinavian Journal of Statistics*, *49*(1), 455–479. https://doi.org/10.1111/sjos.12523

Rapanta C., Botturi L., Goodyear P., Guàrdia L., & Koole M. (2020). Online university teaching during and after the COVID-19 crisis: Refocusing teacher presence and learning activity. *Postdigital Science and Education*, *2*(3), 923–945. https://doi.org/10.1007/s42438-020-00155-y

Rempała G. A. (2023). Equivalence of mass action and poisson network SIR epidemic models. *Biomath*, *12*(2), 2311237. https://doi.org/10.55630/j.biomath.2023.11.237

Rennert L., Kalbaugh C. A., Shi L., & McMahan C. (2020). Modelling the impact of presemester testing on COVID-19 outbreaks in university campuses. *BMJ Open*, *10*(12), e042578. ISSN 2044-6055. https://bmjopen.bmj.com/content/10/12/e042578. https://doi.org/10.1136/bmjopen-2020-042578

Rennert L., McMahan C., Kalbaugh C. A., Yang Y., Lumsden B., Dean D., Pekarek L., & Colenda C. C. (2021). Surveillance-based informative testing for detection and containment of SARS-CoV-2 outbreaks on a public university campus: An observational and modelling study. *The Lancet Child & Adolescent Health*, *5*(6), 428–436. ISSN 2352-4642. https://www.sciencedirect.com/science/article/pii/S2352464221000602. https://doi.org/10.1016/S2352-4642(21)00060-2

Schnell P. M., Wascher M., & Rempala G. A. (2024). Overcoming repeated testing schedule bias in estimates of disease prevalence. *Journal of the American Statistical Association*, *119*(545), 1–13. https://doi.org/10.1080/01621459.2023.2238943

Shah M., Ferra G., Fitzgerald S., Barreira P. J., Sabeti P. C., & Colubri A. (2022). Containing the spread of mumps on college campuses. *Royal Society Open Science*, *9*(1), 210948. https://doi.org/10.1098/rsos.210948

Walke H. T., Honein M. A., & Redfield R. R. (2020). Preventing and responding to COVID-19 on college campuses. *JAMA*, *324*(17), 1727–1728. https://doi.org/10.1001/jama.2020.20027

Wang X., Du Z., Johnson K. E., Pasco R. F., Fox S. J., Lachmann M., McLellan J. S., & Meyers L. A. (2021). Effects of COVID-19 vaccination timing and risk prioritization on mortality rates, United States. *Emerging Infectious Diseases*, *27*(7), 1976. https://doi.org/10.3201/eid2707.210118

Zhang X., Wu J., Smith L. M., Li X., Yancey O., Franzblau A., Dvonch J. T., Xi C., & Neitzel R. L. (2022). Monitoring SARS-CoV-2 in air and on surfaces and estimating infection risk in buildings and buses on a university campus. *Journal of Exposure Science & Environmental Epidemiology*, *32*(5), 751–758. https://doi.org/10.1038/s41370-022-00442-9